

SUPPLEMENTARY INFORMATION

## Hydrogen Cycling in $\gamma$ -Mg(BH<sub>4</sub>)<sub>2</sub> with Cobalt-based Additives

O.Zavorotynska<sup>a</sup>, I. Saldan,<sup>a,b</sup> S. Hino,<sup>a,1</sup> T. D. Humphries,<sup>a</sup> S. Deledda,<sup>a</sup> B.C. Hauback<sup>\*,a</sup>

<sup>a</sup>Physics Department, Institute for Energy Technology, P.O. Box 40, NO-2027 Kjeller, Norway

<sup>b</sup>Department of Physical and Colloid Chemistry, Ivan Franko National University of Lviv,  
6 Kyryla and Mefodia Str., UA-79005 Lviv, Ukraine

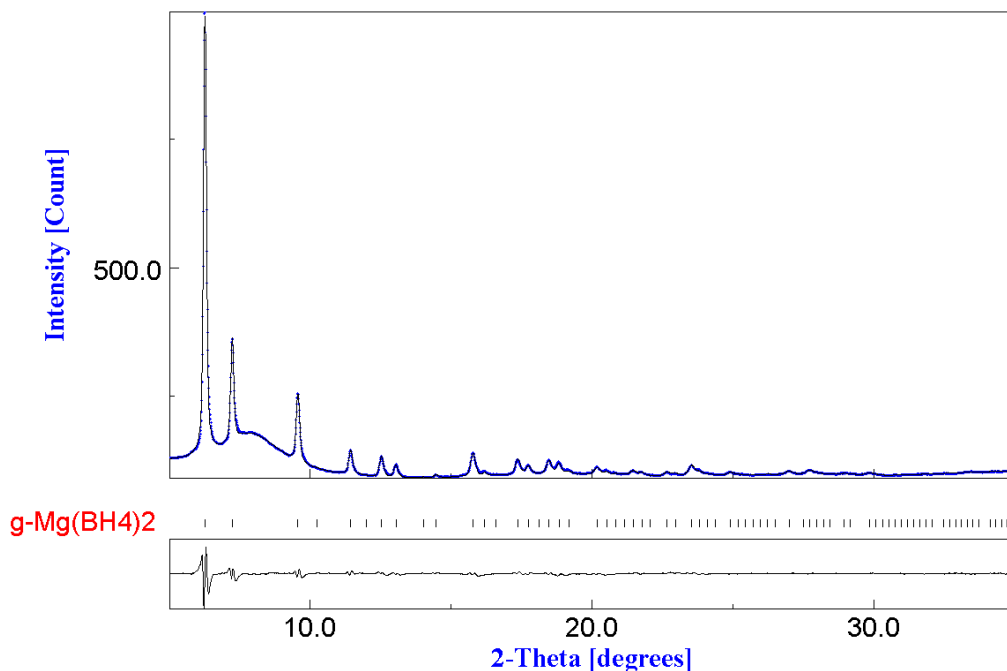


Fig. S1. SR-PXD ( $\lambda = 0.70135 \text{ \AA}$ ) pattern of the commercial milled Mg(BH<sub>4</sub>)<sub>2</sub> (S1) showing only  $\gamma$ -phase and a small amount of amorphous phase(s).

<sup>1</sup> Current affiliation: Graduate School of Engineering, Hokkaido University, Sapporo, 060-8628, Japan

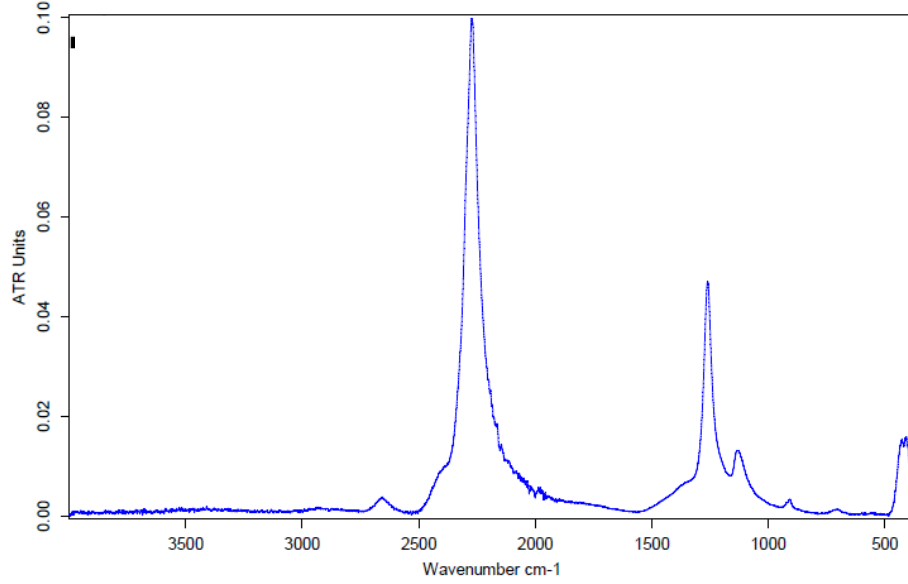


Fig. S2. IR-ATR spectrum of commercial  $\gamma$ -Mg(BH<sub>4</sub>)<sub>2</sub> used for sample preparation (S0).

Table S1. Solid-state reaction models<sup>1</sup> (general equation and the equation for  $y=0.5$  at  $t=t_{0.5}$ ) used for comparison with the experimental desorption and absorption curves (Fig. 2). The curves shown on Fig. 2 were plotted according to the numerical data for  $y$  and  $t/t_{0.5}$  reported in ref. S1 (ref.33).

Short name	Equation	Description
D1	$D_1(y) = y^2 = \frac{k}{x^2}t; D_1(0.5) = 0.2500\left(\frac{t}{t_{0.5}}\right)$	1-dimensional diffusion-controlled reaction with constant diffusion coefficient, where $2x$ is the thickness of the reacting layer
D2	$D_2(y) = (1 - y)\ln(1 - y) + y = \frac{k}{r^2}t = 0.1534\left(\frac{t}{t_{0.5}}\right)$	2-dimensional diffusion-controlled reaction into a cylinder of radius $r$
D3	$D_3(y) = (1 - (1 - y)^{1/3})^2 = \frac{k}{r^2}t = 0.0426\left(\frac{t}{t_{0.5}}\right)$	3-dimensional diffusion-controlled reaction in a sphere of radius $r$
D4	$D_4(y) = \left(1 - \frac{2y}{3}\right) - (1 - y)^{2/3} = \frac{k}{r^2}t = 0.0367\left(\frac{t}{t_{0.5}}\right)$	Diffusion-controlled reaction starting on the exterior of a spherical particle of radius $r$
R2	$R_2(y) = 1 - (1 - y)^{1/2} = \frac{u}{r}t = 0.2929\left(\frac{t}{t_{0.5}}\right)$	Phase-boundary controlled reaction at the interface, for a circular disk reacting from the edge inwards, or for a cylinder, where $u$ is a constant velocity of the interface

R3	$R_3(y) = 1 - (1 - y)^{1/3} = \frac{u}{r}t = 0.2063\left(\frac{t}{t_{0.5}}\right)$	Phase-boundary controlled reaction at the interface, for a sphere of radius $r$ , reacting from the surface inward, where $u$ is a constant velocity of the interface
A2	$A_2(y) = (-\ln(1 - y))^{\frac{1}{2}} = kt = 0.8326t/t_{0.5}$	Avrami-Erofe'ev equation for two dimensional growth of random nuclei with constant interface velocity
A3	$A_3(y) = (-\ln(1 - y))^{\frac{1}{3}} = kt = 0.8850(t/t_{0.5})$	Avrami-Erofe'ev equations for three dimensional growth of random nuclei with constant interface velocity

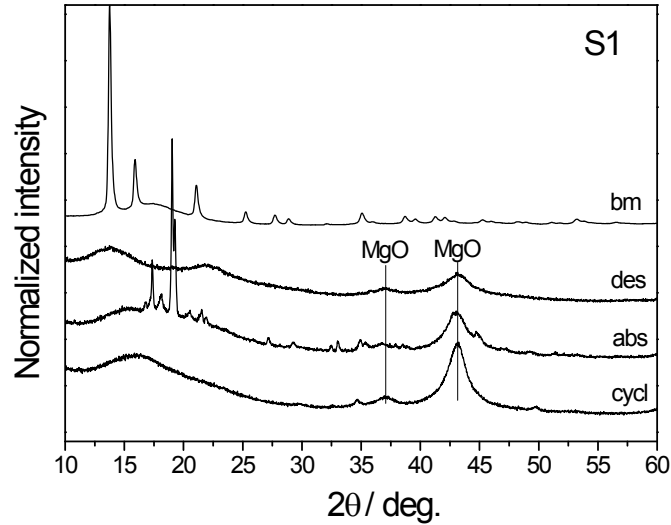


Fig. S3. PXD patterns of the S1 before (*bm*) and after desorption (*des*), after the 1<sup>st</sup> absorption (*abs*), and the 3<sup>rd</sup> absorption (*cycl*). ( $\lambda = 1.5418 \text{ \AA}$ ).

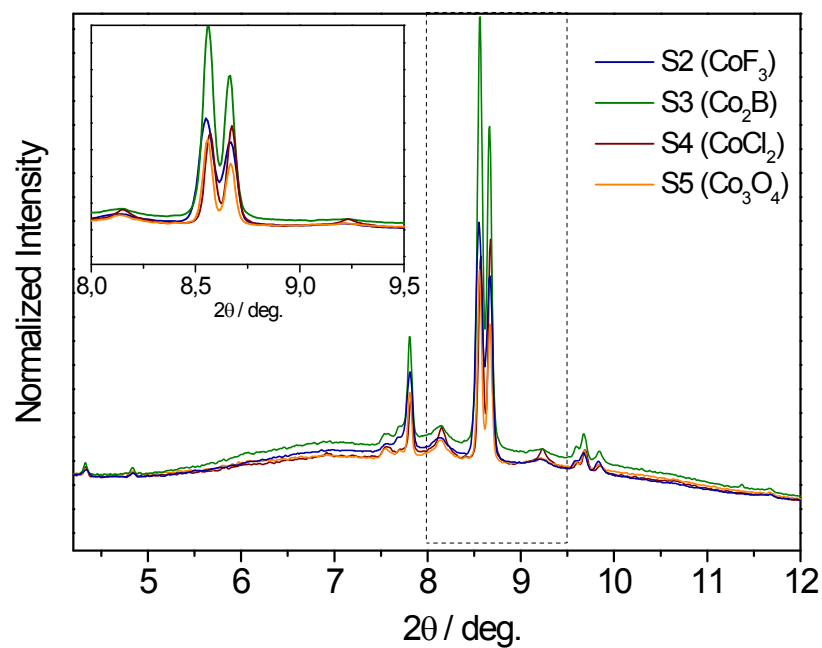


Fig. S4. SR-PXD patterns of samples S2-S5 after the 1<sup>st</sup> absorption. The inset shows the expanded view of the  $\text{Mg}(\text{BH}_4)_2$  peaks in the 8.0 - 9.5° region. ( $\lambda = 0.70135 \text{ \AA}$ ).

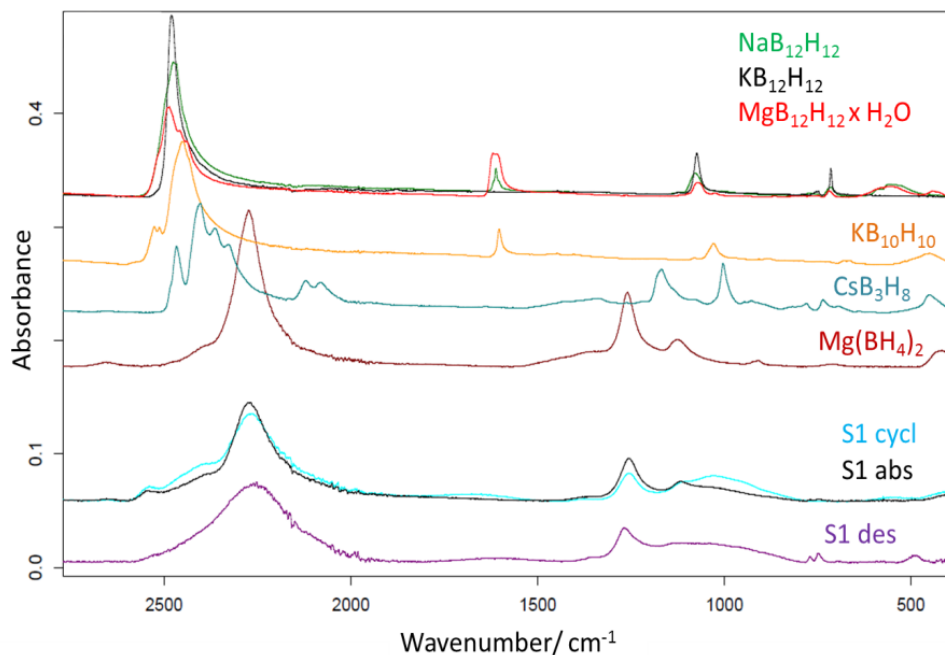


Fig. S5. ATR-IR spectra of S1 after the first desorption, 1<sup>st</sup> absorption, and cycling compared to the spectra of some reference compounds. The peaks at  $\nu_{\text{max}}/\text{cm}^{-1}$  1630 in the spectra of  $\text{MB}_{12}\text{H}_{12}$  ( $\text{M} = \text{Mg}, \text{Na}$ ) and  $\text{KB}_{10}\text{H}_{10}$  are due to water.

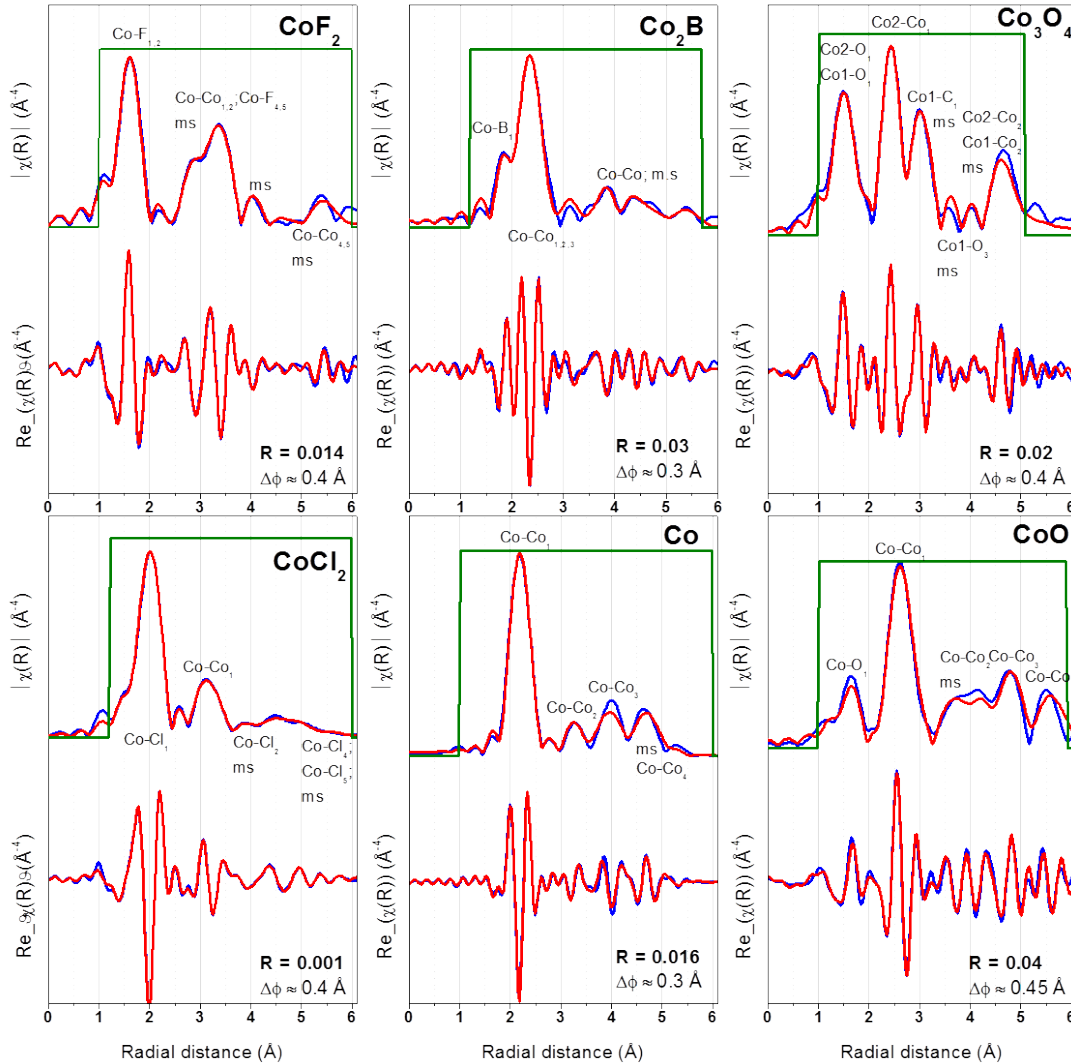


Fig. S6. Amplitude (up) and real part (bottom) of the  $k^3$ -weighted FT of the EXAFS spectra of the commercial additives that were used as references, and peak assignment. Fit quality  $\mathbf{R}$  and phase shift  $\Delta\phi$  are reported on the figures. Experimental data are plotted in blue, fit – in red, and fitting window – in green. **CoF<sub>2</sub>**: The assignment was based on the fit to the 25 theoretical single scattering (ss) and multiple scattering (ms) paths. Only the largest contributing backscattering neighbors are indicated on the figure. Several less significant multiple scattering paths at the larger  $R$  (4.5 – 6 Å) were omitted, which is the reason of the somewhat worse fit in this region. The parameters of the fit were: passive electron reduction factor  $S_0^2$ , shift in the edge energy  $\Delta E_0$ , mean square displacement  $\sigma^2$ , and changes in the lattice parameters.  $\sigma^2$  for the multiple scattering paths was expressed through the respective values for the single scattering

paths involving the same scatters.<sup>2</sup>  $\Delta R$  was expressed through the lattice parameters minus  $R_{eff}$ , where the latter is the initial interatomic distance. **Co<sub>2</sub>B**: Fit of the 13 theoretical ss and ms paths in the range 1.17-5.7 Å. Due to the complexity of the structure, several less significant multiple scattering paths were omitted which is the reason of larger errors. This fit however still satisfies our purposes of peak assignment. The parameters of the fit were: passive electron reduction factor  $S_0^2$ , shift in the edge energy  $\Delta E_0$ , mean square displacement  $\sigma^2$ , and changes in the lattice parameters.  $\sigma^2$  for the multiple scattering paths was expressed through the respective values for the single scattering paths involving the same scatters.  $\Delta R$  was expressed through the lattice parameters minus  $R_{eff}$ , where the latter is the initial interatomic distance. **CoCl<sub>2</sub>**: fit of 10 ss and ms pathways with parameters  $S_0^2$ ,  $\Delta E_0$ ,  $\sigma^2$ ,  $\Delta R$ . **Co<sub>3</sub>O<sub>4</sub>**: fit of 17 ss and ms pathways with parameters  $S_0^2$ ,  $\Delta E_0$ ,  $\sigma^2$ ,  $\alpha$ ,  $\Delta a$ . The fit was performed based on two FEFF calculations for the Co1 (Co<sup>2+</sup>, tetrahedral coordination, 1/3 of atoms) and Co2 (Co<sup>3+</sup>, octahedral coordination, 2/3 atoms).  $S_0^2$  for Co2 was expressed as  $S_0^2(1)*2$ .  $\Delta R$  was expressed through  $R_{eff}*\alpha$  for multiple scattering pathways and through the cell parameter  $a$  ( $a = a_0 + \Delta a$ ) for the single scattering pathways. The misfit results from the omitting of some less significant ms pathways and also probably from some slight differences between the crystallographic structure and the Co<sub>3</sub>O<sub>4</sub> sample used in this work. **CoO**: fit of 25 ss and ms pathways with parameters  $S_0^2$ ,  $\Delta E_0$ ,  $\sigma^2$ ,  $\alpha$ .  $\Delta R$  was expressed through  $R_{eff}*\alpha$ . The misfit results from the omitting of some less significant ms pathways and also probably from some slight disorder in the CoO sample. The latter is especially true for the fit of the first two peaks where all theoretical pathways are included in the model. **Co**: fit of 28 ss and ms pathways with parameters  $S_0^2$ ,  $\Delta E_0$ ,  $\sigma^2$ ,  $\alpha$ .  $\Delta R$  was expressed through  $R_{eff}*\alpha$ .

## References

- S1. J. H. Sharp, G. W. Brindely and B. N. Narahari Achar, *J. Am. Ceram. Soc.*, 1966, **49**, 379-382.
- S2. E. A. Hadson, P. G. Allen, L. J. Terminello, M. A. Denecke and T. Reich, *Phys. Rev. B: Condens. Matter*, 1996, 156-165.